Computational materials design and engineering

C. J. Kuehmann* and G. B. Olson

Computational materials design integrates targeted materials process–structure and structure–property models in systems frameworks to meet specific engineering needs. Design inherently consists of many competing requirements that require judicious decisions regarding key tradeoffs. The goal of computational materials design is to apply the best scientific understanding to facilitate decisions regarding the optimal tradeoffs that meet desired needs in the most time and resource efficient manner. Mechanistic materials design models require adequate fidelity to determine the favourability of one design solution over another but also the ability to be extrapolated over large parameter space to search for design optima in unexplored terrain. Design processes must not only efficiently find optimal solutions, but quickly identify failures. More broadly, materials design can only be as successful as the ability to identify the correct requirements for an application, and those requirements must address not only performance but also qualification hurdles including prediction of manufacturing variation.

Keywords: Computational modelling, Materials design, Accelerated qualification

Introduction

The application of systems engineering principles, utilising computational materials science, allows the rapid and efficient development of design solutions for materials with specific application requirements. The general application of the technique has been well developed in other references.[1–4] Expansion of computational materials design for the qualification and implementation of new materials into engineering systems was established by the US Defence Advanced Research Projects Agency (DARPA) Accelerated Insertion of Materials (AIM) programme.[5] Following up on these efforts, the US Office of Naval Research has partnered with DARPA and established the Digital 3-D (D-3D) initiative creating the next generation computational and analytical tools to support computational materials engineering incorporating the AIM methodology.[6]
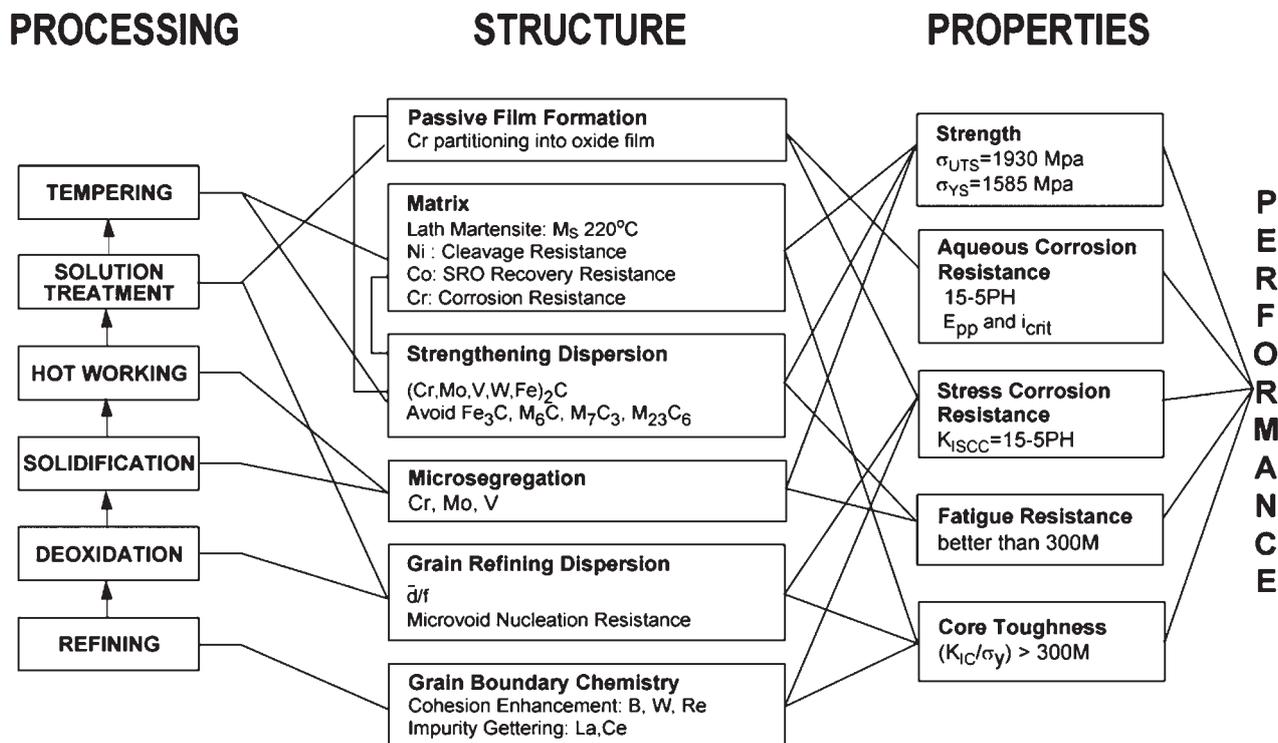
The driver for an engineering approach to materials design is meeting a specific need for materials performance in the context of a system. Such a perspective necessitates the focus of the design activity on the wider context of the application. Combinations of properties must be considered within specified process, cost, environmental and life cycle constraints. Tradeoffs are inherent in the approach and tools to effect the design must address the optimisation of such tradeoffs explicitly. An example of the systems approach is contained in Fig. 1 for ultrahigh strength corrosion resistant steel.

The performance of the alloy is embodied in the combination of properties outlined in the column on the right. The design process determines suitable microstructural concepts to meet these property goals, as indicated by the middle column. Available processing paths to access the microstructural objectives are quantified in the left column. The links between the subsystem blocks in the flow block diagram represent process–structure and structure–property models required to quantitatively design an alloy to meet the desired performance objectives.

The DARPA AIM programme extended the use of computational modelling into the challenges of scale up and materials qualification and certification. In the context of classical materials development, AIM applies to materials discovered experimentally in the laboratory and addresses the significant failure rate of such materials during scale-up and qualification. Applying advanced computational modelling to scale-up, AIM accelerates and reduces the risk associated with producing new materials reliably at scale. In addition, the programme addressed the issue of establishing quantitative estimates of material property variation used for component design. Currently, such variation is quantified by expensive and time consuming statistical experimentation. AIM applies a predictive probabilistic approach that integrates limited experimental data with computational materials modelling to efficiently establish variability. In the pilot programme, AIM methods quantified the strength variation experienced in the production of 1000 turbine discs with as few as 15 individual measurements.[7] In the context of computationally designed materials, AIM becomes even more effective since mechanistic modelling directly applicable

QuesTek Innovations LLC, 1820 Ridge Ave., Evanston, IL, USA

*Corresponding author, email ckuehmann@questek.com

PROCESSING   STRUCTURE   PROPERTIES

PROCESSING
- TEMPERING
- SOLUTION TREATMENT
- HOT WORKING
- SOLIDIFICATION
- DEOXIDATION
- REFINING

STRUCTURE

Passive Film Formation
Cr partitioning into oxide film

Matrix
Lath Martensite: M_S 220°C
Ni : Cleavage Resistance
Co: SRO Recovery Resistance
Cr: Corrosion Resistance

Strengthening Dispersion
$(Cr,Mo,V,W,Fe)_2C$
Avoid Fe_3C, M_6C, M_7C_3, $M_{23}C_6$

Microsegregation
Cr, Mo, V

Grain Refining Dispersion
$\bar{d}/f$
Microvoid Nucleation Resistance

Grain Boundary Chemistry
Cohesion Enhancement: B, W, Re
Impurity Gettering: La,Ce

PROPERTIES

Strength
σ_{UTS}=1930 Mpa
σ_{YS}=1585 Mpa

Aqueous Corrosion Resistance
15-5PH
E_{pp} and i_{crit}

Stress Corrosion Resistance
K_{ISCC}=15-5PH

Fatigue Resistance
better than 300M

Core Toughness
(K_{IC}/σ_y) > 300M

PERFORMANCE

1 Flow block diagram for ultrahigh strength corrosion resistant steel indicates desired property objectives, microstructural subsystems and sequential processing steps needed for design: links between systems blocks indicate quantitative models needed to affect design via science based computation

to the material is already available and scale issues can be initially incorporated into design considerations.

The ONR/DARPA D-3D initiative is applying lessons learned in the DARPA AIM programme to establish the next generation of modelling and characterisation tools enabling AIM adoption. The programme is further focusing on modelling approaches to incorporate three-dimensional considerations, including orientation and clustering effects, into key modelling components. New experimental techniques to quantify three-dimensional characteristics are being developed to efficiently calibrate and validate these new modelling tools.[8]

Computational materials modelling for design

Computational materials models for design purposes differ significantly from those used in traditional materials science research activities. While conventional computational materials science modelling strives to understand general phenomena, design models are used to control a materials system and optimise it for a specific outcome. Computational materials design models are used to make specific engineering decisions and tradeoffs, i.e. is option A more advantageous than option B? Their fidelity depends on the type of question being asked. Models used in a conceptual design exercise need less absolute accuracy than those employed in the design of a detailed embodiment, but they also must be fast to allow a large design space to be explored. Design models must also extrapolate well, requiring a strong mechanistic foundation. By definition, a new design will be outside the known parameter space on which a model is based. Lastly, design models need to be highly cooperative. A given design will have many, often

conflicting, requirements. A number of models will need to be employed and operated cooperatively to determine the best combinations of process and composition to meet a diverse set of material objectives.

Figure 2 illustrates five stages of development in computational materials design and AIM development: conceptual, parametric, embodiment, detailed and qualification. The lower portion of the diagram depicts the modelling activities that are associated with each of the five stages as well as some typical modelling tools that may be employed. Table 1 defines some of these modelling tools, identifies the methods underlying them and provides information on specific software implementations that are available. The upper portion of Fig. 2 describes prototyping and production activities typical to the five stages of design and development, as well as examples of specific experimental techniques applied to them.

In the conceptual phase, general questions about mechanistic aspects of the alloy are addressed. What strengthening mechanisms should be deployed? And, given the answer, what microstructures, phases and components are the most beneficial? Here, general materials science tools are very helpful. CALPHAD models of thermodynamics and mobility can determine relative phase stabilities, individual component solubilities and rate constants given sufficient (often concurrent) database development. If thermodynamic relationships are not available, or the literature lacks sufficient experimental data to create them, first principles *ab initio* techniques can be used to calculate formation energies, magnetic states and lattice parameters for candidate structures. This very basic level of 'phase engineering' can be quite productive when identifying new constituents to mimic particular mechanisms in a new alloy system that may have been
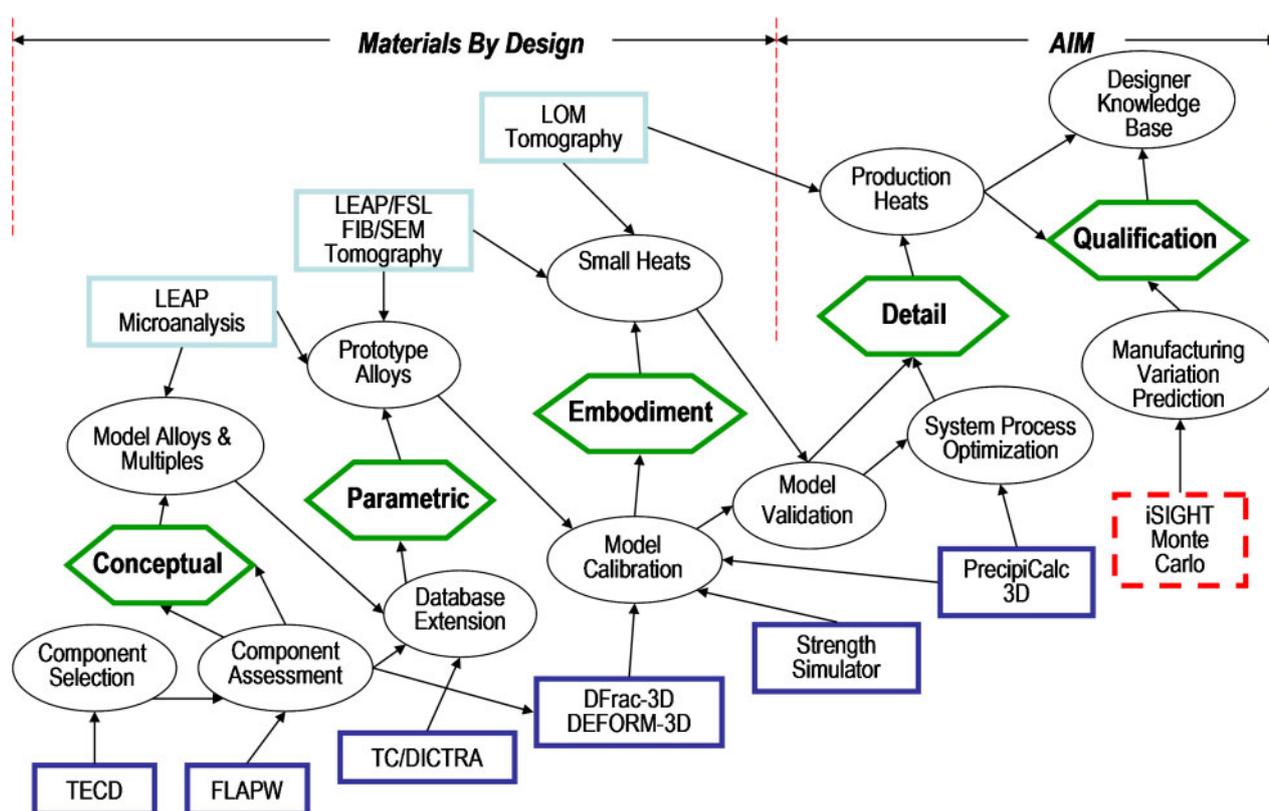
2 Five stages of development in computational materials design include conceptual, parametric, embodiment and detailed design phases as well as materials qualification: details above each stage represent experimental efforts and specific analytical tools involved in validating design; details below each stage indicate computational modelling approach and specific tools employed in creating design

well studied and characterised in another. General analytical models for mechanistic process–structure relationships are very applicable in the conceptual phase where rough estimates of required microstructural features are needed to establish feasibility of particular concepts. For example, analytical relations for Orowan strengthening or particle shearing can be used to estimate phase fractions and particle sizes needed for efficient precipitation strengthening. CALPHAD models of equilibrium or metastable thermodynamics can then determine if such phase fractions and particles sizes are possible. Model alloys can be produced and characterised to determine the validity of the mechanistic assumptions on which a given concept is based in order to establish overall feasibility and enhance fundamental parameters.

Table 1 Listing of available methods and models used in computational materials design and engineering including available software platforms

Method/model	Description	Tools
TECD	Topological electron charge density (TECD) analysis uses charge density input from pseudopotential or full electron DFT methods to visualise gradients, critical points and other features in the charge density of atomic polyhedra	TECD is available from the Molecular Theory Group at the Colorado School of Mines, Golden, CO, USA.
FLAPW	The fully linearised augmented plane wave (FLAPW) method is an all electron implementation of density functional theory (DFT) that allows the calculation of total energy and electronic structure for given crystal structures	The code QMD-FLAPW is maintained and supplied by Quantum Materials Design Inc. The code WEIN2k is available from the Vienna University of Technology. The Flair Consortium and the FLEUR project are other variants
CALPHAD	CALculation of PHase and Alloy Diagrams (CALPHAD) is a technique that uses various models of the composition and temperature dependence of the free energy of phases to calculate equilibrium and metastable states of multicomponent systems	ThermoCalc is available from ThermoCalc Software, Stockholm, SE. Pandat is available from CompuTherm LLC, Madison, WI USA. FactSage is available from CRCT, Montreal, CA and GTT-Technologies, Aachen, DE
DICTRA	DICTRA is an extension of CALPHAD specific to the ThermoCalc platform that incorporates atomic mobility and uses finite difference methods to solve 1-D diffusion and moving boundary problems	DICTRA is available from ThermoCalc Software, Stockholm, SE

In the parametric design phase, individual design models, representing the links in Fig. 1, are first combined to attempt an optimisation of the materials system as a whole. Again simpler models for phase stability, solubility and mechanistic analytical process–structure relationships are employed, in this case to establish if the conflicting requirements of the design can be accommodated with a judiciously chosen set of design parameters. Here the model predictions may be parameterised and normalised to the design objective set by the design requirements. This exercise tests the design tradeoffs of conflicting requirements, and determines if suitable flexibility exists to meet all requirements simultaneously. Because these parameterised (or parametric) models typically predict trends well but may have limited accuracy, a carefully chosen set, usually less than six, of design solutions, is prototyped to maximise the likelihood of spanning an acceptable design. The characterisation of these prototypes is completed to directly validate design assumptions and model accuracy as much as to strictly demonstrate the achievement of design goals.

Using the results from the parametric designs, computational models and fundamental parameters are updated and expanded to increase accuracy and incorporate additional complexity in the embodiment design phase. Where a parametric design may use driving force and precipitation rate constants to define precipitate microstructures, the embodiment design phase typically employs more rigorous precipitation simulations to define precipitate distributions, using numerical implementations of nucleation, growth and coarsening.[9] Strength modelling may move from mechanistic analytical models to explicit simulations of dislocation dynamics.[10] Simple phase stability considerations may move to multicomponent diffusional simulations of moving boundary problems with tools like DICTRA. The first considerations of manufacturing scale are addressed utilizing full scale processing conditions and rates in these simulation based process–structure and structure–property calculations. The goal of the embodiment design is to determine a unique design optimum with as much accuracy as possible. Prototypes at this stage are again used to validate the mechanistic underpinnings of the design but are also intended to be a very accurate representation of the design when produced at scale.

Detailed design considerations complete the computational design approach for a material and transition into qualification aided by AIM methods. Here computational modelling is used to further specify the full range of conditions that may be required for an engineering material. Intermediate states and processing considerations are further developed and may include modelling annealed states of the material to address issues such as machinability or formability. Forging process parameters and windows may be determined from incipient melting considerations or phase stability. Compatibility with secondary processing such as surface treatments may also be modelled and optimised. The detailed design phase fully completes the design and considers the total life cycle of the material from the first processing step involved in its manufacture to the last step in its disposal or recycling.

The qualification phase demonstrates the ability of the material to meet requirements in a component with a high level of confidence. Here AIM methods integrate computational modelling and targeted experiments to rapidly determine minimum material performance from production processes. Figure 3 demonstrates the method conceptually in which Monte Carlo simulations of material performance are performed using the expected distribution of processing parameters to produce a modelled dataset that contains the intrinsic shape of the property distribution due to known sources of variation. A limited experimental dataset is then used to translate the modelled distribution to match the mean and width of the experimental measurements. The resulting modified distribution is then used to estimate the minimum material properties. This method allows minimum properties to be predicted well before adequate experimental data would exist to do so.

Examples of computation in design

The best example of a commercial alloy created by this methodology is the Ferrium S53 (AMS 5922) corrosion resistant landing gear steel allowing a drop in replacement for current non-stainless landing gear steels, eliminating the need for cadmium plating.[11] As depicted in the flow block diagram in Fig. 1, the S53 alloy is a secondary hardening steel strengthened by efficient M_2C carbide precipitates and contains sufficient Cr content to provide passivation against general corrosion. Grain boundary chemistry is controlled to maximise cohesion, leading to excellent SCC resistance. The sequential processing steps experienced by the alloy are depicted on the left most column of the flow block diagram and are constrained to existing processes for steels employed in current structural aircraft applications to maximise manufacturability. The subcomponents of this system are connected by process–structure and structure–property relationships, representing the mechanistic modeling tools necessary to employ quantitative computational design.

The application of the system flow-block diagram in conjunction with the computational models begins with identification of key design trade offs. Key to achieving the stated design goals is the development of an efficient strengthening dispersion. M_2C carbide is an efficient strengthener in steels due to its high modulus misfit with BCC Fe and its ability to precipitate coherently at the nanoscale. It is important to note that the coherency leads to significant complications in predicting the precipitation kinetics as the coherency strain energy must be accommodated in the precipitation model. This has been well studied and reported in the literature[4,12,13] and such models were utilised in Fig. 4 where the overall precipitation driving force and the normalised coarsening rate constant are reported as a function of Mo and V content in the S53 alloy.

This design calculation maximises the resulting strength through the precipitation driving force, while assuring this strength can be achieved with reasonable tempering parameters. Maintaining adequate martensite kinetics to ensure a martensitic alloy while achieving high strengthening is another key design tradeoff. Quantitative martensite kinetic models[14] are used to predict the martensite start temperature along with the M_2C precipitation driving force in Fig. 5 as a function of Co and Ni contents.
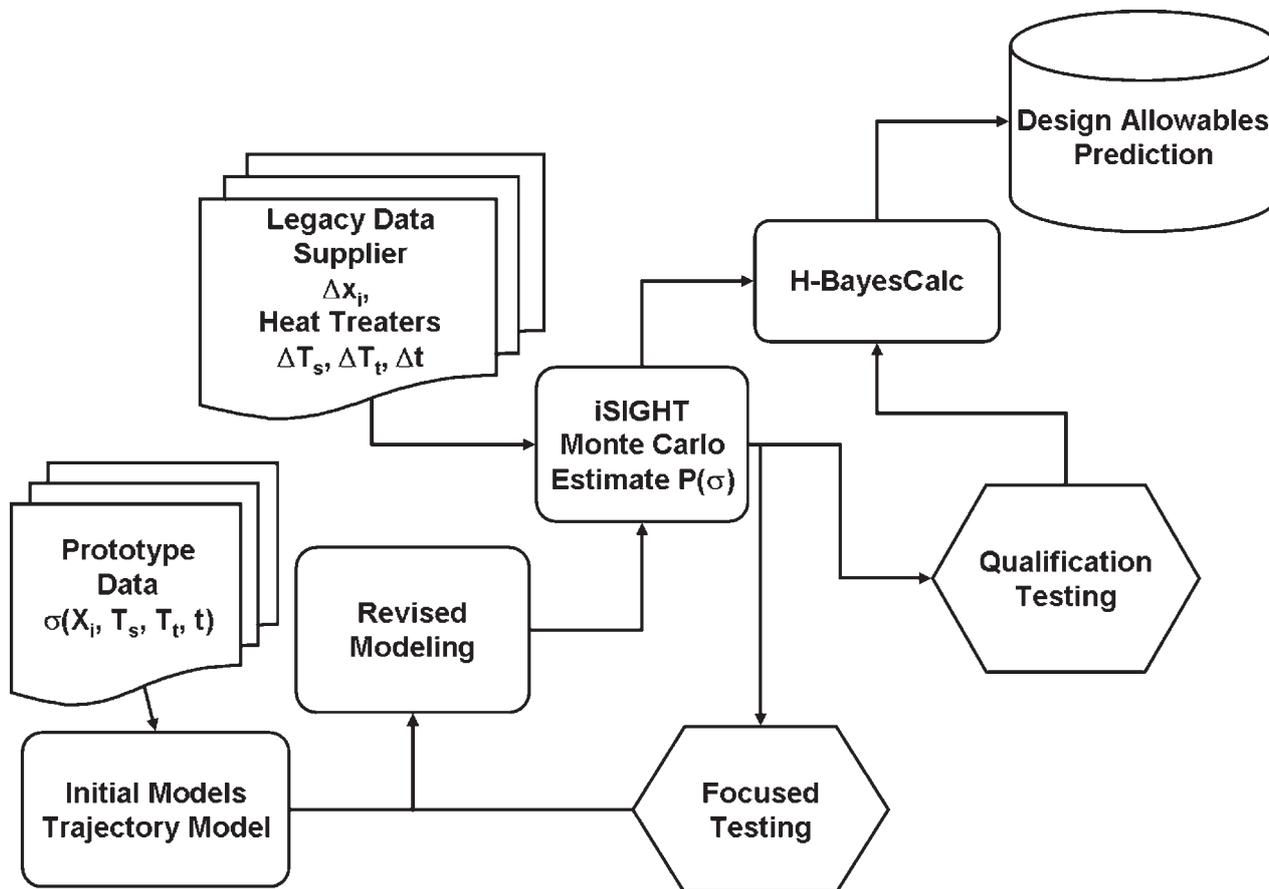
3 AIM method integrates modelling with targeted experimental data to produce design allowable minimum properties using anticipated supplier process variation estimates

This chart allows achieving maximum strengthening while requiring a sufficiently high M_S temperature to maintain a predominantly martensitic alloy.

Design for corrosion utilised the results of Campbell and Olson[4] modelling the stability of passivating films in secondary hardening alloys. The analysis utilises
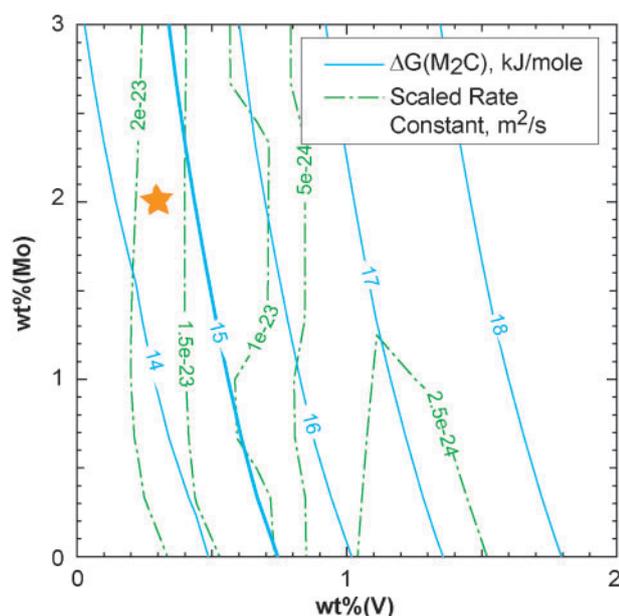
4 Maximizing M_2C driving force while maintaining normalised coarsening rate for adequate tempering kinetics provides a secondary hardening alloy with highly efficient strengthening: S53 alloy achieves greater than 1930 MPa tensile strength with only 0·2 wt-% carbon
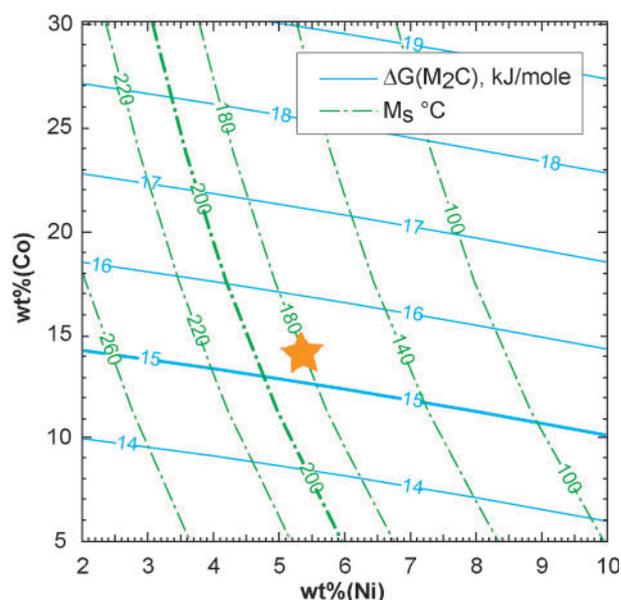
5 Maintaining sufficiently high M_S temperature while maximising carbide driving force allows efficient strengthening in fully martensitic alloy: contours of M_2C precipitation driving force overlaid with alloy M_S temperature determine optimal Co and Ni contents
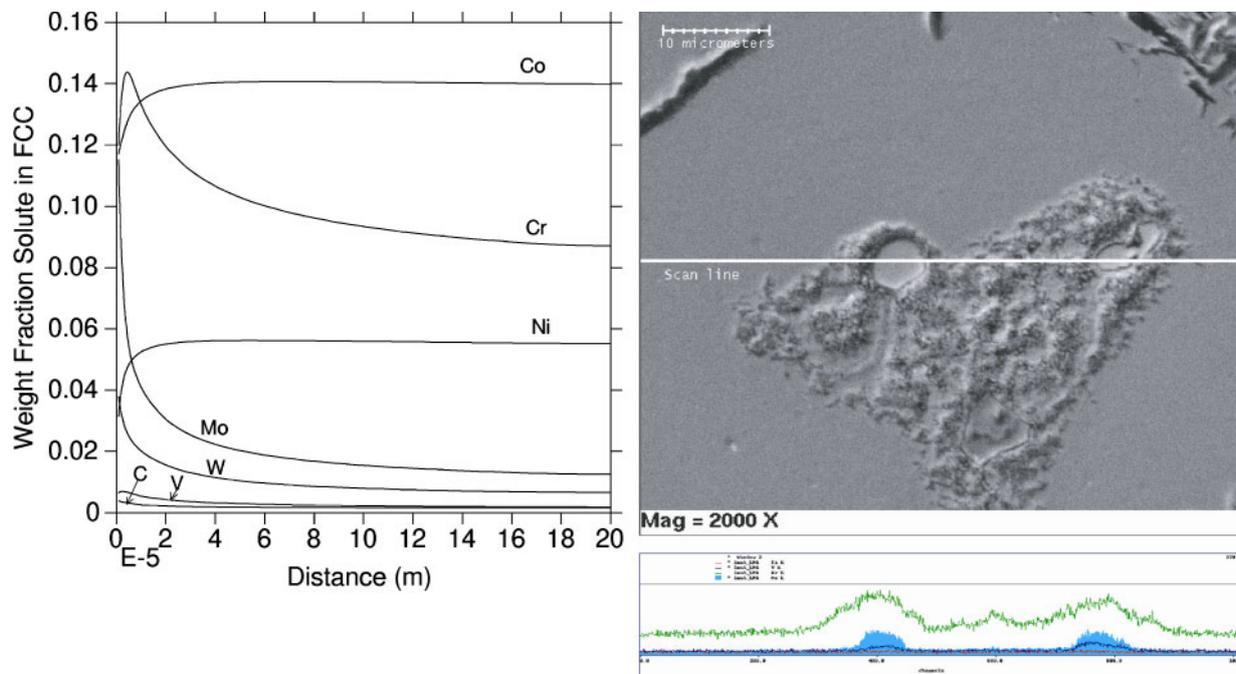
6 One-dimensional multicomponent diffusion simulations of solidification of S53 alloy indicate extent of segregation that can be expected in final ingot: this segregation is verified qualitatively from SEM observations of ingot material

multicomponent thermodynamic effects to maximise Cr partitioning in the spinel oxide primarily driven by Co content. In addition, the nanoscale M_2C carbides are designed to be sufficiently small compared to the oxide scale to enable their oxidation during passivation, freeing the Cr contained in these carbides to incorporate into the passive film.

Additional constraints on ductile fracture, grain boundary chemistry and grain pinning dispersions are used to complete the design optimisation and uniquely identify the alloy composition that represents the best compromise of the diverse design goals and constraints. Grain boundary chemistry considerations are applied based on first principles calculations of impurity and alloying effects of the interfacial cohesion of BCC high angle grain boundaries.[15] The grain pinning dispersion design was based on calculations of the TiC/Fe interfacial adhesion that demonstrated excellent resistance to microvoid formation.[16]

Full scale processing concerns were also integrated into the design. Candidate design compositions were used in solidification simulations using one-dimensional multicomponent diffusion simulations employing DICTRA.[17] The results of these simulations in Fig. 6 show the segregation profiles across secondary dendrite arms expected during large scale production of ingots using typical VAR processing conditions. These findings were later validated from actual production ingots.

Of greater importance is the ability to homogenise expected solidification segregation with commercially acceptable thermal treatments. Figure 7 shows DICTRA predictions of homogenisation of Mo in the as cast ingot of the S53 alloy at 1350°C as a function of time. The simulation guides processing recommendations and indicates that sufficient homogenization can be reached in reasonable processing windows.

Extending use of computation to qualification and implementation

AIM methods were applied to the prediction of the ultimate tensile strength of S53, the primary design objective of the alloy. The goal of this exercise was to predict property design minimums, which normally require 10 heats and 300 individual observations, using only three heats and 30 individual observations. A computational model employed predictions of the M_2C precipitate size as a function of composition and processing, as well as the resulting strength when accounting for additional contributions from solid solution, martensite substructure and dislocation density effects. Using expected process variation, a large dataset with over 300 simulations was produced. This distribution was then scaled to fit 20 experimental data points spanning two heats using a linear transformation function determined by the best fit. This analysis indicated that the 1% minimum ultimate tensile strength was predicted to be 1920 MPa, below the 1930 MPa design goal. This early indication allowed additional process optimisation to be completed, increasing the ultimate tensile strength by an additional 10 MPa. The analysis was repeated with 30 data produced from three heats of the alloy and is shown in Fig. 8a (and showing a prediction of 1930 MPa). The resulting full dataset of 10 heats and over 600 individual observations is shown in Fig. 8b. The AIM prediction is within 7 MPa of the 1% minimum tensile strength statistically defined by the 10 heats of data. In this AIM example, if data development had proceeded and the property deficit was discovered when the full dataset was complete, over a year of development and in excess of $500 000 would have to be repeated to meet the property goals.
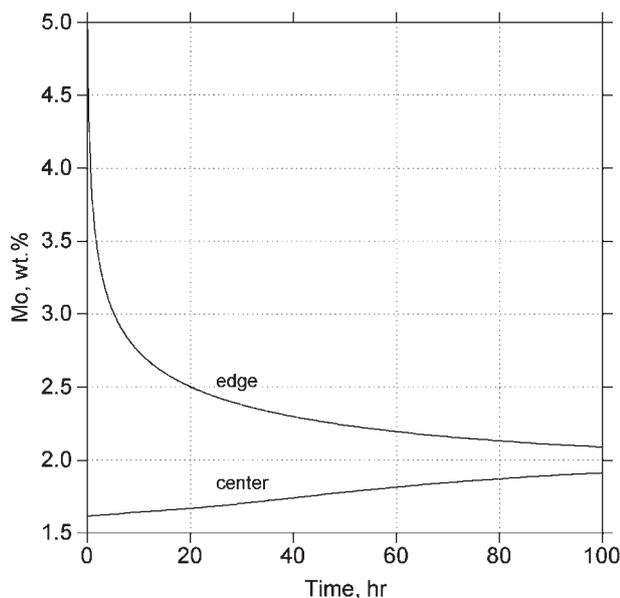
7 Homogenisation of Mo segregation in S53 alloy as function of time at 1350°C: two curves represent composition of Mo at dendrite centre and edge, and initial profiles are provided by solidification simulations from Fig. 6

Conclusion

In summary, the example of the S53 steel (AMS 5922) demonstrates how computational materials design enabled the development of a complex multicomponent alloy that targeted properties enabling a drop-in replacement for Cd plated ultrahigh strength steels by a corrosion resistant alternative. The S53 design employs efficient M_2C strengthening in a fine ductile lath martensite matrix. The matrix contains sufficient Cr for passivation that is further enhanced by matrix Co that increases the Cr activity to levels greater than common 12 wt-%Cr steels. Grain boundary chemistry is controlled to maximise grain boundary cohesion and to avoid SCC and H embrittlement. Additionally, grain pinning particles were designed to be an effective pinning dispersion while minimising the impact on microvoid formation during ductile fracture. The computational techniques employed here accomplished the ambitious S53 design in three design prototype test iterations and represented a significant cost and time savings over traditional empirical development techniques.

Acknowledgements
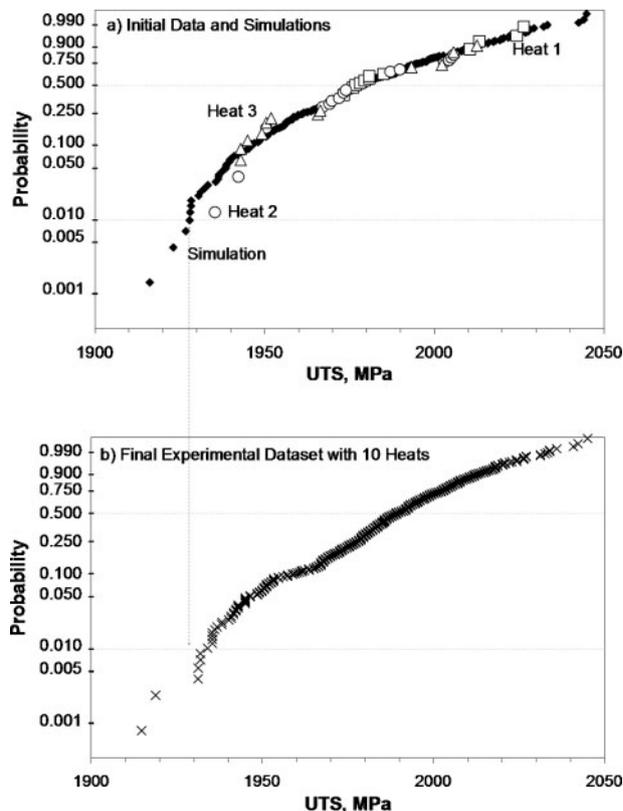
8 *a* AIM analysis of ultimate tensile strength of S53 using simulation results and 30 data from three individual heats agrees well with completed dataset from 10 heats and *b* over 600 observations in determining 1% minimum design allowable

References

1. G. B. Olson: *Science*, 1997, **277**, 1237.
2. G. B. Olson: *Science*, 2000, **288**, 993–998.
3. A. Saha and G. B. Olson: *J. Comput. Aided Mater. Des.*, 2007, **14**, 177.
4. C. E. Campbell and G. B. Olson: *J. Comput. Aided Mater. Des.*, 2000, **7**, 145–170.
5. Committee on Accelerating Technology Transition, National Research Council: 'Accelerating technology transition: bridging the valley of death for materials and processes in defense systems'; 2004, Washington, DC, The National Academies Press.
6. F. Vernerey *et al.*: *JOM*, 2006, **58**, 45–51.
7. D. G. Harlow: *Eng. Fract. Mech.*, 2007, **74**, 2943–2951.
8. A. C. Lewis *et al.*: *JOM*, **58**, 52–56.
9. H.-J. Jou, P. W. Voorhees and G. B. Olson: in 'Superalloys 2004', 887–886; 2004, Warrendale, PA, TMS.
10. V. Mohles: *Philso. Mag. A*, 2002, **81A**, 971–990.
11. C. J. Kuehmann, B. E. Tufts and P. Trester: *Adv. Mater. Process.*, 2008, **166**, 37–40.
12. K. C. King, P. W. Voorhees and G. B. Olson: *Metall. Trans. A*, 1991, **22A**, 2199–2210.
13. G. Ghosh, G. B. Olson and C. E. Campbell: *Metall. Trans. A*, 1999, **30A**, 501–512.
14. G. Ghosh and G. B. Olson: *Acta Metall. Mater.*, 1994, **42**, 3391.
15. W. T. Geng, A. J. Freeman and G. B. Olson: *Phys. Rev. B*, 2001, **63B**, 165415.
16. J.-H. Lee, T. Shishidou, Y.-J. Zhao, A. J. Freeman and G. B. Olson: *Philos. Mag.*, 2005, **85**, 3683–3697.
17. H. Lippard, C. E. Campbell, U. P. David, G. B. Olson, T. Björklind, U. Borggren and P. Kellgren: *Metall. Trans. B*, 1998, **29B**, 205–210.